This article has been accepted for publication in a future issue of this journal, but has not been fully edited. Content may change prior to final publication. Citation information: DOI 10.1109/TPWRS.2022.3141794, IEEE Transactions on Power Systems

# Quantum Distributed Unit Commitment: An Application in Microgrids

Nima Nikmehr, *Senior Member, IEEE,* Peng Zhang, *Senior Member, IEEE* and Mikhail A. Bragin, *Member, IEEE*

***Abstract*—The dawn of quantum computing brings on a revolution in the way combinatorially complex power system problems such as Unit Commitment are solved. The Unit Commitment problem complexity is expected to increase in the future because of the trend toward the increase of penetration of intermittent renewables. Even though quantum computing has proven effective for solving a host of problems, its applications for power systems' problem have been rather limited. In this paper, a quantum unit commitment is innovatively formulated and the quantum version of the decomposition and coordination alternate direction method of multipliers (ADMM) is established. The above is achieved by devising quantum algorithms and by exploiting the superposition and entanglement of quantum bits (qubits) for solving subproblems, which are then coordinated through ADMM to obtain feasible solutions. The main contributions of this paper include: 1) the innovative development of a quantum model for Unit Commitment; 2) development of decomposition and coordination-supported framework which paves the way for the utilization of limited quantum resources to potentially solve the large-scale discrete optimization problems; 3) devising the novel quantum distributed unit commitment (QDUC) to solve the problem in a larger scale that currently available quantum computers are capable of solving. The QDUC results are compared with those from its classical counterpart, which validate the efficacy of quantum computing.**

***Index Terms*—Quantum computing, Quantum distributed optimization, Unit commitment, Microgrids.**

## I. Introduction

Unit commitment (UC) [1] is a critically important problem for the operational optimization within power systems. Within the UC problem, the presence of binary commitment decision variables leads to combinatorial complexity. Moreover, with the goals to increase the penetration of intermittent renewables, the complexity is expected to increase in the future and the new sources for disruptive solution methodologies need to be found.

**General Discussion on Quantum Computing.** A very promising and quickly emerging technology, which has the potential to efficiently handle combinatorial complexity in the future is based on quantum computing (QC), which has already proved promising to overcome computational difficulties faced by classical computers in solving a variety of problems arising in biomedical science, weather forecasting, risk analysis [2], aerospace engineering [3], cybersecurity [4], chemistry [5], and machine learning [6]. To efficiently perform the quantum algorithms, an appropriate design of quantum circuit running sequentially the quantum gates on the existing qubits is required for implementation of problems [7].

**Quantum Optimization.** Universal quantum computers with up to 1,000 qubits are expected to be produced in this decade [8], which will allow the researchers to solve large-scale optimization problems which cannot be solved by classical counterparts. Even though current quantum optimization algorithms are inchoate and can only handle relatively small optimization problems and problems of certain types [9], significant progress has been made to solve combinatorial optimization problems. Currently available quantum optimization algorithms can already solve problems formulated as quadratic unconstrained binary optimization (QUBO) problems. One of the first quantum optimization algorithms is the Quantum Approximate Optimization Algorithm (QAOA) [10] where a multi-level parameterized quantum circuit is established to optimize the expected value of the QUBO objective function. Another quantum optimization algorithm is Grover's algorithm [11], which was used for the portfolio optimization problem, formulated in a QUBO form. One of the first attempts to show the superiority of QC over classical computing in optimization problems refers to the combinatorial problem of bounded occurrence Max E3LIN2 [12], in which the QAOA beats the existing best approximation bound for efficient classical algorithms. Another advantage of QC over classical computing is realized in Grover's algorithm, in which a quadratic speed-up was achieved on a unstructured search problem as an optimization problem. In this problem, we are aiming at locating an item among a large list of items with a unique property [13]. In [14], the researchers have proven that the query complexity on Grover's problem is achievable using the class of QAOA circuits. The QAOA was used to solve the maximum cut (max-cut) combinatorial problem [15]. In a recent promising research, Egger, et al [16], have improved the performance of QAOA in solving max-cut problem as a continuous relaxations of NP-Hard combinatorial optimization problem. In their algorithm, namely warm-starting quantum optimization, Goemans-Williamson random hyperplane rounding for max-cut problem can find cuts whose expected value is at least as good as classical approximations at any circuit depth.

Although, the aforementioned quantum optimization algorithms have been exploited to solve binary optimization problems, large-scale problems cannot be solved because of limited number of qubits currently available. Moreover, quantum optimization methods are not naturally distributed in a sense that the coordination of distributed entities is not supported. Furthermore, while the large-scale quantum computers will exist in a foreseeable future, their availability will likely be costly

This work was supported in part by the Advanced Grid Modeling Program under Department of Energy's Office of Electricity, in part by the National Science Foundation under Grant No. OIA-2040599, and in part by Stony Brook University's Office of the Vice President for Research through a Quantum Information Science and Technology Seed Grant. This research used resources of the Oak Ridge Leadership Computing Facility, which is a DOE Office of Science User Facility supported under Contract DE-AC05-00OR22725.

N. Nikmehr and P. Zhang are with the Department of Electrical and Computer Engineering, Stony Brook University, Stony Brook, NY 11794, USA (e-mail: p.zhang@stonybrook.edu).

Mikhail A. Bragin is with the Department of Electrical and Computer Engineering, University of Connecticut, Storrs, CT 06269, USA.

This article has been accepted for publication in a future issue of this journal, but has not been fully edited. Content may change prior to final publication. Citation information: DOI 10.1109/TPWRS.2022.3141794, IEEE Transactions on Power Systems

and limited. To enable the efficient use of smaller quantum computers to solve large-scale problems, a decomposition and coordination framework is required.

**Decomposition and Coordination Methods.** To coordinate distributed entities, such as units within the Unit Commitment problem, decomposition and coordination methods have been used [17], [18]. The alternate direction method of multipliers (ADMM) is used to overcome the combinatorial complexity issues faced by Augmented Lagrangian Relaxation (ALR) method. Within the ADMM, subproblems are smaller in size and are easier to solve than the relaxed problem within ALR [19]. In [20], ADMM aims at dualizing the power flow constraints between the neighboring regions in UC optimization problem. In [21], the Surrogate Lagrangian Relaxation (SLR) method is used to solve large-scale security-constrained unit commitment (SCUC) problems with multiple combined cycle units without requiring the "so-called" optimal dual value for convergence. These methods enable the decomposition into several smaller subproblems so that the resulting mixed-binary optimization (MBO) problems are solvable by quantum methods. This direction is promising and opens a new window to solve a wide range of optimization problems in power systems by using current quantum algorithms.

The main contribution of the paper is to develop a quantum algorithm with futuristic implications to efficiently solve optimization problems, and the improvement of convergence of ADMM, which is a classical aspect, is out of the scope of the paper. Accordingly, the main focus is on the development of decomposition and coordination-supported framework for quantum optimization, which allows to solve problems larger that currently available quantum computers are capable of solving. The implications of the new method are thus profound. In Section II, the unit commitment problem is formulated in a QUBO form amenable for quantum optimization in a novel way. In Section III, the QAOA is presented for the quantum UC problem. The quantum-inspired Alternate Direction Method of Multipliers is presented in subsection III.B. In Section IV, it is demonstrated that distributed UC problem can take advantage of QC compared to the classical counterpart. In Section V, the quantum computing capabilities and current limitations are discussed.

## II. Unit Commitment Problem Formulation

In this section, the traditional Unit Commitment problem is presented first. The novelty of this section is then to reformulated the UC problem in a QUBO form amenable for quantum optimization.

### A. Unit Commitment Formulation

Within the UC problem, the generation cost is minimized subject to unit-wise constraints (e.g., generation capacity, ramp-rated, minimum up/down time, etc) as well as the system-wide constraints (e.g., system demand, reserve, transmission capacity, etc.)

**Objective function.** The following objective function consisting of the total fuel cost ($\mathcal{F}(P)$) and the total commitment cost ($\mathcal{G}(u)$) should be minimized [22]:

$$\min_{P,u} \; OF = \min_{P,u} \; \left[\mathcal{F}(P) + \mathcal{G}(u)\right]. \tag{1}$$

where, $\mathcal{F}(P)$ and $\mathcal{G}(u)$ can be written as follows:

$$\mathcal{F}(P) = \sum_{t\in T}\sum_{i\in I}\left[\alpha_i \cdot P_{t,i}^2 + \beta_i \cdot P_{t,i} + \gamma_i\right], \tag{2a}$$

$$\mathcal{G}(u) = \sum_{t\in T}\sum_{i\in I}\omega_i \cdot u_{t,i}. \tag{2b}$$

where, $P_{t,i}$ is the generation level of $i^{th}$ unit at hour $t$ and $\alpha_i$, $\beta_i$ and $\gamma_i$ are fuel price parameters of $i^{th}$ unit. For the commitment cost $\mathcal{G}(u)$ including startup and shutdown costs, the binary decision variable $u_i \in \{0,1\}$ is the commitment status of unit $i$ at hour $t$. The commitment price of each unit including startup/shutdown price, is denoted by $\omega_i$. Also, the sets $T$ and $I$ denote time period and generation unit, respectively.

**Constraints:** The objective function is subject to the following constraints:

$$\mathcal{D} \cdot u \leq D, \tag{3a}$$

$$\mathcal{J} \cdot P \leq J, \tag{3b}$$

$$\mathcal{Q} \cdot u + \mathcal{R} \cdot P \leq Y. \tag{3c}$$

where, constraint (3a) includes any constraints associated with the binary variable $u$, e.g., startup and shutdown constraints, minimum up time and minimum down time. Constraint (3b) is associated with power generation variable $P$, e.g., spinning reserves, ramping rate, transmission lines, and power balance limits. It is noted that the power balance can be described as two opposite inequalities. Additionally, constraint (3c) includes both binary variable $u$ and non-binary variable $P$ to demonstrate the minimum and maximum generation capacity limit.

In the following, the UC problem formulation amenable for quantum computing will be developed in a novel way.

### B. Quantum Formulation of Unit Commitment

Within this subsection, a background information behind quantum optimization will be presented first. Then the quantum UC will be formulated.

*1) Preliminary discussion on quantum optimization:* Unlike classical computers, where information is represented by using binary bits (0 or 1), quantum computers use the so-called "quantum bits" - qubits. A qubit is a superposition of states $|0\rangle$ and $|1\rangle$. The superposition can take either a value of 0 or 1 with a certain probability after a measurement. One qubit can thus hold two bits of information. Likewise, 2 qubits are a superposition of four entangled states $|0,0\rangle$, $|0,1\rangle$, $|1,0\rangle$ and $|1,1\rangle$, and so on. Therefore, $n$ qubits hold $2^n$ bits of information. The main idea behind the quantum computers is to exponentially reduce the complexity as compared to the classical computers. To perform the calculation on the quantum platform, within the so-called quantum circuit, quantum gates are used as computational blocks. In a quantum circuit, input qubits are first initialized by using equiprobable states. Qubits are then passed through quantum gates to rotate the entangles states within each qubit, which essentially updates the probability of each state. Ultimately, the state of the qubit is measured, and the states with higher probabilities appear in the measurement more often.

As established in [23], a solution to a QUBO problem is equivalent to the ground state of a corresponding Ising

This article has been accepted for publication in a future issue of this journal, but has not been fully edited. Content may change prior to final publication. Citation information: DOI 10.1109/TPWRS.2022.3141794, IEEE Transactions on Power Systems

Hamiltonian. Several methods were developed to establish the Hamiltonian of the Ising model [24]. We firstly discuss a general procedure behind creating Ising Hamiltonian for any QUBO optimization problems, and then, the procedure is applied to the UC problem. To define the Ising model, a graph $G = (V, \varepsilon)$ with vertices set $V$ and edges set $\varepsilon$ is commonly used (shown in Fig. 1). The Hamiltonian Ising model is then built based upon the existing vertices $V$ and their connected edges $\varepsilon$ between the two vertices. The vertices are physical qubits of the system in which interaction between qubits is realized by $L_{kj}$ while the edges correspond to the possible locations of two-qubit gates. Also, the external magnetic $q_k$ causes a rotation of vertex $V$ with spin $\zeta = \pm 1$. From quantum computing point of view, at any given time, the quantum state $|\psi\rangle$ is described by a vector in the Hilbert space which should be projected to the basis of eigenfunctions of the position operator to prepare the wave function. To reach the ground state, the projected quantum state should be rotated using the spin operators. The quantum state and accordingly wave function is changed after each rotation. It is noted that the rotation operators are linear and unitary operators, and determining the optimized rotation angles lead the system toward the ground state, which is equal to minimum cost function in the optimization problems. In Section III-A, the quantum mechanism to update the rotation angles in the quantum optimization algorithm is explained. The Hamiltonian of the Ising model, which is referred as cost Hamiltonian, is written as follows to find the ground state or minimum energy configuration [25]:

$$\mathcal{H} = \sum_{k=1}^{N} \sum_{j=1, j\neq k}^{N} L_{kj} \cdot \zeta_k^w \cdot \zeta_j^w + \sum_{k \in V} q_k \cdot \zeta_k^w. \tag{4}$$

The first term of the cost Hamiltonian (4) has to do with the interaction of two qubits or vertices of a system, while the second term defines the impact of magnetic field with a spin on each single qubit. The role of edges and vertices in a real quantum circuit will be discussed in further detail in the next section. The total number of spins is defined by $N$, which is the same as the number of vertices. The minimal eigenvalues or ground state of the Ising model (4) is achievable through searching for spins $\zeta_k^w$. Therefore, the optimal rotation angles of spin operators guarantee the optimal values of decision variables, and thereby optimal solution of the optimization problems.

As the physics rule, the ground state is called the most stable state. Thus, the lowest energy state of Hamiltonian of Ising model (4) is the stable state of a system. Accordingly, in optimization problems, quadratic unconstrained binary optimization is the energy function that its corresponding Hamiltonian Ising model should be obtained using a simple conversion [26]. In (4), replacing the spin $\zeta$ by a binary variable $a$ results a QUBO problem. The interaction between spins and external magnetic field acting on a spin in (4) are accordingly changed to $M$ and $r$, respectively:

$$\mathcal{H} = \sum_{(k,j)\in\varepsilon} M_{kj} \cdot a_k \cdot a_j + \sum_{k \in V} r_k \cdot a_k + c. \tag{5}$$

where, $c$ is a constant value and has no impact on the efficiency of the computation. The relation between a spin $\zeta_k$ and a binary variable $a_k$ is derived as follows [27]:

$$a_k = \frac{1 + \zeta_k}{2}, \ k \in V. \tag{6}$$

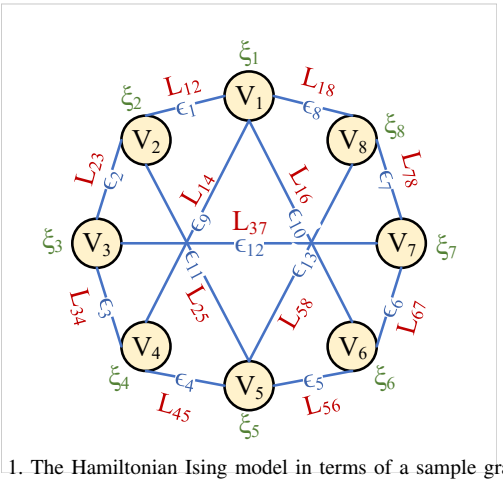


Fig. 1. The Hamiltonian Ising model in terms of a sample graph

*2) Quantum Formulation of Unit Commitment:* To prepare the UC problem for quantum-oriented optimization problem, the objective function (1) should be mapped to the Ising model using the existing relationship between a spin and a binary variable (6). Before going through the Hamiltonian Ising model steps, the UC problem should satisfy the requirements of a QUBO problem, in which the quadratic objective function should include the existing constraints. Thus, several steps should be considered for converting the quantum UC problem to a QUBO problem. To this end, firstly, the generic form of UC constraints (3a), (3b) and (3c) is changed in each step of conversion, and then the specific form of constraints undergo the corresponding changes. To solve the UC problem using a typical quantum variational approach, the quantum states of the problem are prepared using the quantum circuit. Then, the quantum states are measured and the expected value of the UC Hamiltonian is obtained for the given quantum states. Afterwards, a classical solver is employed to find the new set of variational parameters. In Section. III-A, a detailed explanation of the hybrid procedure of the quantum variational approach will be discussed. While in previous quantum optimization methods, only binary and integer variables could be considered in a problem, this paper resolves this issue to make the UC problem industrially practical and cost-effective by assigning continuous variables to DERs generation level. To this end, the developed quantum distributed method is a promising step in solving large scale optimization problems by using QC. In the slack-based formulation, the following three conversion rules are considered to convert the problem into a QUBO:

- The inequality constraints (3a), (3b), and (3c) needs to be converted to an equality constraint first, by using non-negative slack variables $S_{t,1}$, $S_{t,2}$ and $S_{t,3}$:

$$\mathcal{D} \cdot u - D + S_{t,1} = 0, \tag{7a}$$
$$\mathcal{J} \cdot P - J + S_{t,2} = 0, \tag{7b}$$
$$\mathcal{Q} \cdot u + \mathcal{R} \cdot P - Y + S_{t,3} = 0. \tag{7c}$$

  After conversion (7a)-(7c), the size of the problem changes so that for each inequality constraint before conversion, a slack variable is added after the conversion.

This article has been accepted for publication in a future issue of this journal, but has not been fully edited. Content may change prior to final publication. Citation information: DOI 10.1109/TPWRS.2022.3141794, IEEE Transactions on Power Systems

- In the second step, in case there are integer variables in the problem, these type of variables are converted to binary variables. To do this, bounded-coefficient encoding is introduced in [28]. In a case study with DERs, before conversion, there are some binary variables for commitment status of DERs, and the same size of integer variables for the generation level of DERs. After converting the integer variables to binary variables, the constraint associated with the minimum and maximum generation capacity of DERs plays an important role. Consequently, for each value of the range, one binary variable should be assigned. It should be mentioned that each binary variable is assigned to a qubit. Therefore, to solve a simplified UC problem integrating many DERs by QAOA, we need many binary variables or qubits, which exceeds the qubits availability in the quantum computers. Nevertheless, the quantum computers are capable of efficiently solving the problem owing to the decomposition feature of the ADMM method, in which the continuous variables are assigned to a classical solver, and therefore, this conversion is skipped in our developed method. Thus, the size of the problem remains the same in our distributed UC problem.
- In the last step, linear equality constraints are added to the objective function by using quadratic penalties. The modified constraints (7a), (7b) and (7c) are considered in the objective function as follows:

$$\begin{aligned}&(\mathcal{D}\cdot u - D + S_{t,1})^2 + (\mathcal{J}\cdot P - J + S_{t,2})^2 \\ &+ (\mathcal{Q}\cdot u + \mathcal{R}\cdot P - Y + S_{t,3})^2.\end{aligned} \tag{8}$$

  These penalty terms are penalized with an appropriate penalty coefficients to ensure that the constraints are satisfied exactly. A more detailed explanations of operationalization of this idea will be presented in subsection III-B.

After converting the UC problem into a QUBO problem, the objective function can be mapped to the Ising model. According to (6), the decision variables of QUBO and spin $\zeta_k$ can be transformed to each other. In other words, the UC objective function including the decision variables can be mapped to the Hamiltonian Ising model via (6). Therefore, in the original objective function of UC, if the decision variables $P_{t,i}$ is replaced by $\frac{1+\zeta_k}{2}$, the Hamiltonian Ising model is achievable as following:

$$\begin{aligned}\mathcal{H}_O =& \sum_{t\in T}\sum_{i\in I}\sum_{k\in V}\sum_{j\in V}(\alpha_i\cdot\frac{1+\zeta_{t,i,k}}{2}\cdot\frac{1+\zeta_{t,i,j}}{2} \\ &+ \beta_i\cdot\frac{1+\zeta_{t,i,k}}{2}+\gamma_i) \\ =& \frac{1}{4}\sum_{t\in T}\sum_{i\in I}\sum_{k\in V}\sum_{j\in V}\alpha_i\cdot(\zeta_{t,i,k}\cdot\zeta_{t,i,j}+\zeta_{t,i,k}+\zeta_{t,i,j}) \\ &+ \frac{1}{2}\sum_{t\in T}\sum_{i\in I}\sum_{k\in V}[(\beta_i\cdot\zeta_{t,i,k})]+c_1.\end{aligned} \tag{9}$$

where, $c_1$ is a constant value.

Similar to (9), the Ising model can be applied to equality and inequality constraints as well [24]. For the constraints of UC problem, each decision variable should be replaced by $\frac{1+\zeta_k}{2}$. Therefore, to map the the UC constraints (7a), (7b) and (7c) to the Ising model, they should be firstly in terms of $(\mathcal{D}\cdot u - D + S_{t,1})^2$, $(\mathcal{J}\cdot P - J + S_{t,2})^2$ and $(\mathcal{Q}\cdot u + \mathcal{R}\cdot P - Y + S_{t,3})^2$, respectively (see eq. (8)). Then, for each term, the following mapping is applicable:

$$\mathcal{H}_{c,1} = \sum_{t\in T}\sum_{i\in I}\sum_{k\in V}\sum_{j\in V}(\mathcal{D}\cdot\frac{1+\zeta_{t,i,k}}{2}+\frac{1+\zeta_{t,i,j}}{2}-D)^2, \tag{10a}$$

$$\mathcal{H}_{c,2} = \sum_{t\in T}\sum_{i\in I}\sum_{k\in V}\sum_{j\in V}(\mathcal{J}\cdot\frac{1+\zeta_{t,i,k}}{2}+\frac{1+\zeta_{t,i,j}}{2}-J)^2, \tag{10b}$$

$$\begin{aligned}\mathcal{H}_{c,3} = \sum_{t\in T}\sum_{i\in I}\sum_{k\in V}\sum_{j\in V}\sum_{l\in V}(&\mathcal{Q}\cdot\frac{1+\zeta_{t,i,k}}{2}+\mathcal{R}\cdot\frac{1+\zeta_{t,i,j}}{2}+ \\ &\frac{1+\zeta_{t,i,l}}{2}-Y)^2.\end{aligned} \tag{10c}$$

The total energy function is represented as a weighted cost function which is the weighted sum of (9), (10a), (10b), and (10c):

$$\mathcal{H} = \mathfrak{H}_1\cdot\mathcal{H}_O + \mathfrak{H}_2\cdot\mathcal{H}_{c,1} + \mathfrak{H}_3\cdot\mathcal{H}_{c,2} + \mathfrak{H}_4\cdot\mathcal{H}_{c,3}. \tag{11}$$

where, $\mathfrak{H}_1$ and $\mathfrak{H}_2$ are the coefficients of total energy function.

After mapping the objective function to the Hamiltonian, the QUBO problem is prepared for quantum optimization algorithms.

## III. Quantum optimization algorithm

In this section, the Quantum Approximate Optimization Algorithm is presented and Quantum Alternate Direction Method of Multipliers is then developed as a heuristic algorithm to solve the distributed UC problem. Specifically, in subsection A, the QAOA is presented. To enhance the scalability of QAOA, the UC problem is decomposed into unit-wise subproblems after relaxing coupling system demand constraints and subproblems are coordinated by updating Lagrangian multipliers in subsection B. In subsection C, the approximation mechanism of QAOA is explained.

### A. QAOA algorithm

The QAOA aims at finding feasible solutions to the QUBO problems by minimizing the expected value of the Hamiltonian developed in the previous section. The expectation is taken with respect to quantum states, which, in turn, are obtained by rotating the initial state that entangles all possible states with equal probabilities. The minimum expected value of the Hamiltonian is obtained by obtaining feasible rotation angles by using a classical optimizer.

The QAOA algorithm aims to obtain the quantum state $|\psi(\overrightarrow{\xi},\overrightarrow{\tau})\rangle$ such that the expected value of UC Hamiltonian

$$E(\overrightarrow{\xi},\overrightarrow{\tau}) = \langle\psi(\overrightarrow{\xi},\overrightarrow{\tau})|\,\mathcal{H}\,|\psi(\overrightarrow{\xi},\overrightarrow{\tau})\rangle\,. \tag{12}$$

is minimized.

According to [10], through the combination of UC Hamiltonian and single qubit Pauli $X$ rotations through the Pauli operator, a measurement of a state $|\psi(\overrightarrow{\xi},\overrightarrow{\tau})\rangle$ is performed. Also, the transverse field Hamiltonian $B$ is defined as follows based on the total number of bits $n$:

$$B = \sum_{i=1}^{n} X_i. \tag{13}$$

This article has been accepted for publication in a future issue of this journal, but has not been fully edited. Content may change prior to final publication. Citation information: DOI 10.1109/TPWRS.2022.3141794, IEEE Transactions on Power Systems

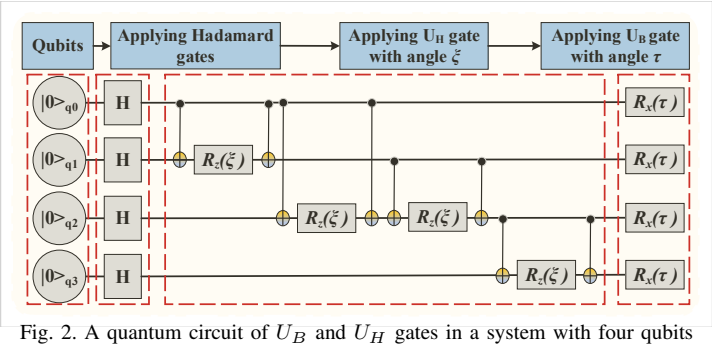


Fig. 2. A quantum circuit of $U_B$ and $U_H$ gates in a system with four qubits

An example of a quantum circuit for 4 qubits is shown in Fig. 2. Before starting the QAOA, a uniform superposition over the $n$ bit-string basis states is initialized as:

$$|+\rangle^n = \frac{1}{\sqrt{2^n}} \sum_{z\in\{0,1\}^n} |z\rangle \,. \tag{14}$$

whereby each state is equiprobable, which is achieved by the using Hadamard gates denoted by the operator $H^{\otimes n}$. To obtain a quantum state $|\psi(\overrightarrow{\xi}, \overrightarrow{\tau})\rangle$ to establish the expectation in (12), the rotation of the entangled state (14) is performed with respect to $\zeta$ through the use of $U_H$ gates, and then the rotation of the resulting state of performed with respect to $\tau$ through the use of $U_B$ gates in the following way:

$$|\psi(\overrightarrow{\xi}, \overrightarrow{\tau})\rangle = U_{B_d} \cdot U_{H_d} \cdot U_{B_{d-1}} \cdot U_{H_{d-1}} \cdots U_{B_1} \cdot U_{H_1} |+\rangle^n \,. \tag{15}$$

where, the operators are in the following explicit forms:

$$U_{B_l} = e^{-i\tau_l B} = \prod_{k=1}^{n} e^{-i\tau_l \zeta_x^k}, \tag{16a}$$

$$U_{H_l} = e^{-i\xi_l H} = \prod_{edge(k,j)} e^{-i\xi_l H^{(k,j)}}. \tag{16b}$$

The number of $U_H$ gates is the same as the number of edges $(k,j) \in \varepsilon$ and the number of $U_B$ gates is the same as the number of vertices in the graph $G$.

The $d$ layers of parametrized $U_B$ and $U_H$ gates are then ready to go through the closed loop optimization process using a classical optimizer. The classical optimizer is then used to obtain variational parameters $\overrightarrow{\xi^*}$ and $\overrightarrow{\tau^*}$ such that the expected function $E$ in (12) is minimized:

$$(\overrightarrow{\xi^*}, \overrightarrow{\tau^*}) = \underset{\overrightarrow{\xi}, \overrightarrow{\tau}}{argmin}\ E(\overrightarrow{\xi}, \overrightarrow{\tau}). \tag{17}$$

The minimum of the expected function $E$ is obtained by running the procedure described above several times, and after each run the state $|(\overrightarrow{\xi}, \overrightarrow{\tau})\rangle$ is measured which return a sample solution $\Upsilon$ with the probability $|\langle\Upsilon|(\xi,\tau)\rangle|^2$. The final purpose of QAOA is to provide an approximation of $|(\xi,\tau)\rangle$ such that the obtained sample $\Upsilon$ reaches the minimum value of objective function. In a sense, the optimization is performed by varying rotation angles $\xi$ and $\tau$ with the intent to obtain a smallest value of the function $E(\overrightarrow{\xi}, \overrightarrow{\tau}) = \langle\psi(\overrightarrow{\xi}, \overrightarrow{\tau})| \mathcal{H} |\psi(\overrightarrow{\xi}, \overrightarrow{\tau})\rangle$ in (12).

The algorithm is summarized in the following steps:

**Step 1)** The initial state $|\psi_0\rangle = |0000\rangle$ with four qubits is passed through a Hadamard gate which results the following $|\psi_1\rangle$ state:

$$|\psi_1\rangle = H^{\otimes 4} \cdot |\psi_0\rangle = \frac{1}{\sqrt{2^4}} \cdot (|0000\rangle + |0001\rangle + \cdots + |1111\rangle). \tag{18}$$

**Step 2)** The controlled-phase gate is applied to state $|\psi_1\rangle$. In controlled-phase gate, a determined phase is added to the target qubit when the control qubit(s) are $|1\rangle$. To show the impact of controlled-phase gate in a 2-qubit system including two controlled-NOT gates and one controlled-phase gate, the $|\psi_2'\rangle$ state is obtained as follows:

$$\begin{aligned} |\psi_2'\rangle &= \underbrace{\begin{bmatrix}1&0&0&0\\0&1&0&0\\0&0&0&1\\0&0&1&0\end{bmatrix}}_{C-NOT gate} \cdot \left( \underbrace{\begin{bmatrix}1&0\\0&1\end{bmatrix}}_{k^{th}\ qubit} \otimes \underbrace{\begin{bmatrix}1&0\\0&e^{-i\xi}\end{bmatrix}}_{j^{th}\ qubit} \right) \cdot \underbrace{\begin{bmatrix}1&0&0&0\\0&1&0&0\\0&0&0&1\\0&0&1&0\end{bmatrix}}_{C-NOT gate} \\ &= \begin{bmatrix}1&0&0&0\\0&e^{-i\xi}&0&0\\0&0&e^{-i\xi}&0\\0&0&0&1\end{bmatrix}. \end{aligned} \tag{19}$$

In (19), a phase change $-\xi$ is applied. According to step 1, the $|\psi_2'\rangle$ state should pass through the Hadamard gate. Therefore, the resultant $|\psi_2\rangle$ state can be obtained on a two-qubit circuit as follows:

$$\begin{aligned} |\psi_2\rangle &= H^{\otimes 2} \cdot |\psi_2'\rangle = \frac{1}{2} \cdot \begin{bmatrix}1&0&0&0\\0&e^{-i\xi}&0&0\\0&0&e^{-i\xi}&0\\0&0&0&1\end{bmatrix} \cdot \begin{bmatrix}1\\1\\1\\1\end{bmatrix} \\ &= \frac{1}{2}\left(|00\rangle + e^{-i\xi}|01\rangle + e^{-i\xi}|10\rangle + |11\rangle\right). \end{aligned} \tag{20}$$

Similarly, for a quantum circuit with four qubits as shown in Fig. 2, the $|\psi_2\rangle$ state is defined as follows:

$$\begin{aligned} |\psi_2\rangle = \frac{1}{4}( &|0000\rangle + e^{-i\xi}|0001\rangle + e^{-3i\xi}|0010\rangle + \cdots \\ &+ e^{-i\xi}|1110\rangle + |1111\rangle). \end{aligned} \tag{21}$$

**Step 3)** Before measurement, the $U_B$ gate with $-\tau$ rotation should be applied to the state $|\psi_2\rangle$. In other words, each qubit should pass through the gate $U_B = \begin{bmatrix} cos(\tau) & -i \cdot sin(\tau) \\ -i \cdot sin(\tau) & cos(\tau) \end{bmatrix}$.

**Step 4)** At the measurement stage, the output of each qubit is extracted based on the $\xi$ and $\tau$. The QAOA should be repeated several times to get the appropriate results for the qubits.

To summarize the execution steps of QAOA, Algorithm 1 gives a brief explanation of creating a quantum circuit for the optimization problem. Additionally, Fig. 3 shows the hybrid nature of QAOA, in which the quantum processor aims at preparing and measuring the quantum state $|\psi(\overrightarrow{\xi}, \overrightarrow{\tau})\rangle$, starting from the initial state. The classical computer processor is employed to update the parameters $\xi$ and $\tau$ for the next iteration. Therefore, there is a feedback loop between the quantum and classical processors in solving a combinatorial optimization problem. In Fig. 4, the hybrid scheme of the QAOA algorithm shows the interaction between classical solver and quantum computing.

In order to efficiently solve the UC problem by using the QAOA presented before, the Alternate Direction Method

This article has been accepted for publication in a future issue of this journal, but has not been fully edited. Content may change prior to final publication. Citation information: DOI 10.1109/TPWRS.2022.3141794, IEEE Transactions on Power Systems

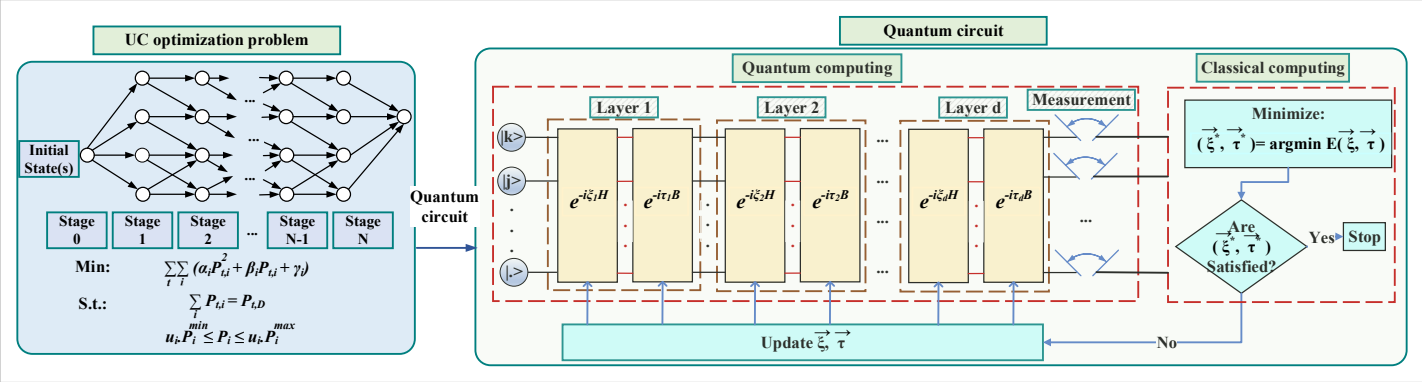


Fig. 3. QAOA framework for UC optimization

**Algorithm 1** Steps of quantum circuit creation for QAOA

**1** Create uniform superposition by applying Hadamard gate.

**2** Apply the $U_H$ gate with angle $\xi$ considering the edges (16b).

**3** Apply $X$ rotation (13) to all qubits with $\tau$ as a angle which results $R_x(\tau)$ (16a).

**4** Measure the computational basis of qubits using $Z$-measurement.

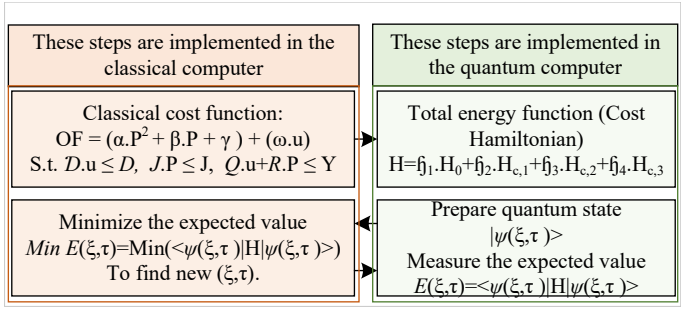


Fig. 4. The hybrid scheme of QAOA

of Multipliers (ADMM) - a decomposition and coordination method - will be presented in the next subsection whereby sub-problems will be solved by using QAOA and then coordinated by updating Lagrangian multipliers.

### *B. Quantum Alternate Direction Method of Multipliers*

In this paper, multi-block decomposition of ADMM is used for the UC problem [29]. In the defined UC problem, the term associated with fuel cost in objective function (1) consists of continuous variables ($P$) for the generation level of DERs. Additionally, in the commitment cost of UC problem, the commitment status of DERs are binary variables ($u$). In the first step, we need to convert the problem to a QUBO form. To this end, firstly the constraint including binary variable (3a) is added to the objective function as an augmented term. Thus, the problem (1) is converted into the following soft-constrained problem in presence of new variable $\breve{z} \in \mathbb{R}$:

$$\underset{u\in U,\breve{z}\in\mathbb{R},P\subseteq\mathbb{R}}{Min} : \mathcal{F}(P)+\mathcal{G}(u)+\frac{\nu_u}{2}\|(\mathcal{D}\cdot u_{t,i}-D)\|_2^2, \quad (22a)$$

$$subject\ to: \mathcal{D}\cdot\breve{z}\le D,\ \mathcal{J}\cdot P\le J,$$
$$\mathcal{Q}\cdot\breve{z}+\mathcal{R}\cdot P\le Y,\ u=\breve{z}. \quad (22b)$$

let $\tilde{P}=[\breve{z}^T,P^T]^T$, $f_0(u)=\mathcal{G}(u)+\frac{\nu_u}{2}\|(\mathcal{D}\cdot u_{t,i}-D)\|_2^2$, and $f_1(\tilde{P}) = \mathcal{F}(P)+\bar{\mathcal{F}}_{\bar{Z}}(\tilde{P})$ where $\tilde{Z} = \{(\breve{z}\in\mathbb{R}, P\subseteq\mathbb{R}) \mid \mathcal{D}\cdot\breve{z}\le D,\ \mathcal{J}\cdot P\le J,\ \mathcal{Q}\cdot\breve{z}+\mathcal{R}\cdot P\le Y\}$.

It is noted that binary and continuous variables are separated in (22a). Therefore, the problem (22a) subject to (22b) is rewritten as following:

$$\underset{u\in U,\tilde{P}\in\mathbb{R}}{Min} : f_0(u)+f_1(\tilde{P}), \quad (23a)$$

$$subject\ to: A_0\cdot u+A_1\cdot\tilde{P}=0. \quad (23b)$$

where, $A_0$ and $A_1$ are the coefficients of variables $u$ and $\tilde{P}$ respectively. The implementation steps of ADMM in multi-block problem is listed as following:

**Step 1:** Initialize the iteration index $s$, decision variables, penalty factor, and stopping criteria.

**Step 2:** Solve the QUBO subproblem to update the corresponding variables:

$$u_i^s = \underset{u\in\{0,1\}}{argmin}\sum_{t\in T}\left[\omega_i\cdot u_{t,i}+\frac{\nu_u}{2}(\mathcal{D}\cdot u_{t,i}-D)^2\right]+ \sum_{t\in T}\lambda_{t,s-1}^T\cdot A_0\cdot u_{t,i}+\sum_{t\in T}\frac{\rho_3}{2}\|A_0\cdot u_{t,i}+A_1\cdot\tilde{P}_{t,i}^{s-1}\|^2. \quad (24)$$

where, the value of penalty factors $\nu_u$ is set to a large number ($10^3$) to ensure that penalized term is forced to be zero. Also, the value of $\rho_3 > \nu_u$ is set to 1001.

**Step 3:** Solve the convex subproblem to update the corresponding variables:

$$\tilde{P}_i^s = \underset{\tilde{P}\in\mathbb{R}}{argmin} f_1(\tilde{P})+\sum_{t\in T}\lambda_{t,s-1}^T\cdot A_1\cdot\tilde{P}_{t,i} + \sum_{t\in T}\frac{\rho_3}{2}\|A_0\cdot u_{t,i}^s+A_1\cdot\tilde{P}_{t,i}\|^2. \quad (25)$$

**Step 4:** Update the dual variables:

$$\lambda_{t,s}=\lambda_{t,s-1}+\rho_3(A_0\cdot u_{t,i}^s+A_1\cdot\tilde{P}_{t,i}^s). \quad (26)$$

**Step 5**: If the stopping criteria satisfies $\|A_0\cdot u_{t,i}^s+A_1\cdot\tilde{P}_{t,i}^s\|\le\epsilon$, then return the optimized values otherwise go to step 2.

This article has been accepted for publication in a future issue of this journal, but has not been fully edited. Content may change prior to final publication. Citation information: DOI 10.1109/TPWRS.2022.3141794, IEEE Transactions on Power Systems

The Lagrangian function of the UC problem is as follows:

$$\begin{aligned} L(\tilde{P},u,\lambda) =& \sum_{t\in T}\sum_{i\in I}\Big[\omega_i\cdot u_{t,i}+f_1(\tilde{P})\Big] \\ &+\sum_{t\in T}\sum_{i\in I}\Big[\frac{\nu_u}{2}(\mathcal{D}\cdot u_{t,i}-D)^2\Big] \\ &+\sum_{t\in T}\sum_{i\in I}\lambda_t^T\Big[A_0\cdot u_{t,i}+A_1\cdot\tilde{P}_{t,i}\Big] \\ &+\sum_{t\in T}\sum_{i\in I}\Big[\frac{\rho_3}{2}\|A_0\cdot u_{t,i}+A_1\cdot\tilde{P}_{t,i}\|^2\Big]. \end{aligned} \tag{27}$$

ADMM, however, generally does not converge. In the dual space, multipliers are not guaranteed to converge to optimal multipliers, and in the primal space, feasible solutions are not guaranteed to be globally optimal.

### C. Approximation Mechanism of QAOA

In this subsection, the approximation mechanism of QAOA, which guarantees the actual optimum of the problem, is discussed [10], [30].

In the classical combinatorial optimization problems, the purpose of optimization is to find a string that minimizes a classical objective function (1) $OF(P):\{+1,-1\}^N$ on $N-bit$ binary strings $P=p_1p_2\dots p_N$. A desired approximation ratio $r(r\leq 1)$ of an approximate optimization algorithm in finding a string $P$ determines the quality of the solution toward the global minimum solution [30]. Therefore, a good approximation ratio leads the approximate optimization algorithm to generate bit-string $P$ (generated power by DERs) so that $OF^{min}=\min\limits_{P} OF(P)$ is achievable with high probability. The approximation ratio of the objective function can be bounded as following:

$$\frac{OF(P)}{OF^{min}}\geq r \tag{28}$$

where, $OF^{min}$ is the minimum value of the objective function.

As it was discussed in subsection III-A, in the quantum approximation, the variational parameters $\overrightarrow{\xi^*}$ and $\overrightarrow{\tau^*}$ are obtained using the classical optimizer such that the expected function $E=\langle\psi(\overrightarrow{\xi},\overrightarrow{\tau})|\,\mathcal{H}\,|\psi(\overrightarrow{\xi},\overrightarrow{\tau})\rangle$ is minimized (see eq.(17)). To achieve an exact optimal value of $E(\overrightarrow{\xi^*},\overrightarrow{\tau^*})$ where the optimized values of $\xi^*$ and $\tau^*$ were obtained using (17), the approximation ratio can be bounded as follows to obtain an estimate of $r$:

$$\frac{E(\overrightarrow{\xi^*},\overrightarrow{\tau^*})}{C'^{min}}\geq r \tag{29}$$

where, in a $d$ layer of quantum circuit, $\lim_{d\to\infty}E(\overrightarrow{\xi^*},\overrightarrow{\tau^*})=C'^{min}$. In this condition, the QAOA algorithm has a guaranteed approximation ratio that can be obtained with polynomial efficiency in the problem size as as a conventional approximate optimization algorithm.

In the QAOA, firstly the samples are taken from trial state $|\psi(\overrightarrow{\xi},\overrightarrow{\tau})\rangle$ in the computational basis. In the UC problem with the Hamiltonian $\mathcal{H}=\sum_{P\in\{0,1\}^n}OF(P)\,|P\rangle\,\langle P|$, single qubit measurements of the state $|\psi_d(\overrightarrow{\xi},\overrightarrow{\tau})\rangle$ in the quantum state basis is repeated. Therefore, this iterative procedure results the sampling estimate of the following:

$$\langle\psi(\overrightarrow{\xi},\overrightarrow{\tau})|\,\mathcal{H}\,|\psi(\overrightarrow{\xi},\overrightarrow{\tau})\rangle=\sum_{P\in\{0,1\}^n}OF(P)|\,\langle P|\psi_d(\overrightarrow{\xi},\overrightarrow{\tau})\rangle\,|^2 \tag{30}$$

In the second step, the obtained string $P$ using the distribution $\langle P|\psi_d(\overrightarrow{\xi},\overrightarrow{\tau})\rangle\,|^2$ is used to assess the cost function $OF$ by taking an average over total samples. Finally, a classical optimization is employed to optimize the $E(\overrightarrow{\xi},\overrightarrow{\tau})$.

To achieve a solution with high probability and close to the optimized expectation value $E(\overrightarrow{\xi^*},\overrightarrow{\tau^*})$, assume that the Hamiltonian $\mathcal{H}$ of UC problem has the total $w$ number of terms in the form of $\mathcal{H}=\sum_{i=1}^{w}\hat{A}_i$ by a universal constant $||\hat{A}_i||\leq\hat{A}$. To obtain $\xi^*$ and $\tau^*$ close to the expected value $E(\overrightarrow{\xi^*},\overrightarrow{\tau^*})$ with high probability, the samples drawn from the distribution $|\,\langle P|\psi_d(\overrightarrow{\xi},\overrightarrow{\tau})\rangle\,|^2$ are important, and if the variance is too high, many samples should be considered. Therefore, we should find the bound of the variance of expected value $E(\overrightarrow{\xi},\overrightarrow{\tau})$ as follows:

$$\begin{aligned} &\langle\psi(\overrightarrow{\xi},\overrightarrow{\tau})|\,\mathcal{H}^2\,|\psi(\overrightarrow{\xi},\overrightarrow{\tau})\rangle-\langle\psi(\overrightarrow{\xi},\overrightarrow{\tau})|\,\mathcal{H}\,|\psi(\overrightarrow{\xi},\overrightarrow{\tau})\rangle^2 \\ &\leq\langle\psi(\overrightarrow{\xi},\overrightarrow{\tau})|\,\mathcal{H}^2\,|\psi(\overrightarrow{\xi},\overrightarrow{\tau})\rangle \\ &=\sum_{i,j=1}^{w}\langle\psi(\overrightarrow{\xi},\overrightarrow{\tau})|\,\hat{A}_i\hat{A}_j\,|\psi(\overrightarrow{\xi},\overrightarrow{\tau})\rangle\leq w^2\hat{A}^2 \end{aligned} \tag{31}$$

As it can be seen from (31), the variance of $E(\overrightarrow{\xi},\overrightarrow{\tau})$ is bounded by $w^2\hat{A}^2$. It means that to achieve a $\xi^*$ and $\tau^*$ close to the expected value $E(\overrightarrow{\xi^*},\overrightarrow{\tau^*})$ with high probability, variance of expected value should be satisfied as (31).

From complexity theory point of view, classically sampling from the output of a general quantum circuit cannot be done efficiently [31]–[33]. Even in small depth quantum circuits (e.g., the lowest quantum circuit depth $d=1$), the classical computers cannot efficiently execute the problems [10] compared to the quantum computers. This feature of QC can lead the quantum optimization algorithms to outperform the classical counterparts in computation time in near-future quantum machines.

## IV. Numerical results

In this section, two case studies are considered. Within the first study, the UC problem including three MGs is solved in a centralized way by using QAOA. Within the the second case study, the distributed coordination between MGs are used to obtain the feasible scheduling of distributed energy resources (DERs). In this paper, to run the optimization problems, IBM Quantum provides the statevector simulator for optimization quantum circuits, and explores their performance under realistic device noise models.

### A. Centralized UC

In the centralized framework, all information of microgrids are sent to a central controller, and then the optimization process is run for the whole network including the MGs' objective function [34]. In Fig. 5, the centralized operation mode of microgrids is depicted where each microgrid control center (MGCC) provides the Ising Hamiltonian model of its objective

This article has been accepted for publication in a future issue of this journal, but has not been fully edited. Content may change prior to final publication. Citation information: DOI 10.1109/TPWRS.2022.3141794, IEEE Transactions on Power Systems

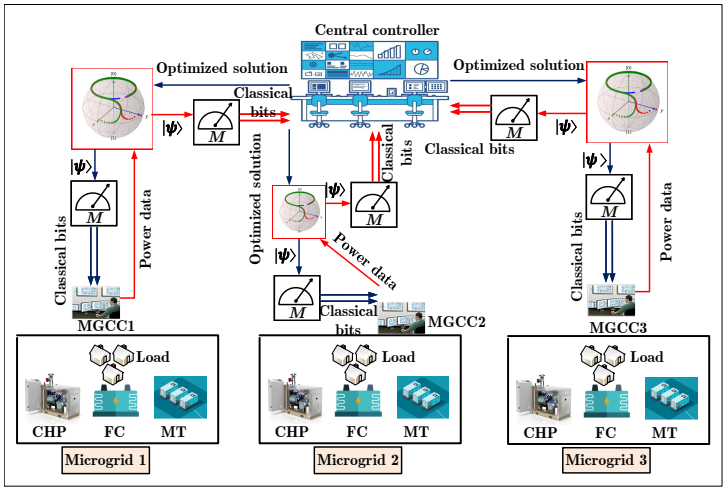


Fig. 5. Centralized operation mode of microgrids

TABLE I. Specifications of DERs in the first scenario of centralized UC

| MG No. | DER No. | $\alpha$ | $\beta$ | $\gamma$ | $P^{min}$ | $P^{max}$ |
|---|---|---|---|---|---|---|
| MG1 | DER1 | 0.03 | 2 | 100 | 1kW | 15kW |
| MG2 | DER1 | 0.02 | 5 | 120 | 1kW | 15kW |
| MG3 | DER1 | 0.025 | 4 | 80 | 1kW | 15kW |

function and constraints to the control center and in return, the control center sends the feasible solution of UC which is the expected value of (12). The measuring units in the end of each MGCC can measure the quantum state and convert it into the classical bits. For the optimization purpose, the QAOA, discussed in Section. III-A, is utilized, and tested on three scenarios.

**First scenario: Three DERs.** Firstly, a small network with three MGs is tested. In this scenario, one DER is devoted to each MG to satisfy the hourly demand of the network shown as Fig. 6. The DERs coefficients are described in Table I. The contributions of MGs in supplying the network demand are described in Table II. The contribution of each DER is defined as the multiplication of commitment status and generated power. The zero value for DERs' contribution means that the DER is in off mode.

The results of Table II indicate that the DER of MG1 is economical to be involved in power generation process. Also, the DER of MG3 has an important role in providing the demand of the network. It is seen that the DER of MG2 is expensive to produce power. In Table III, the total operation cost of MGs obtained by QC is compared with those from classical solver,

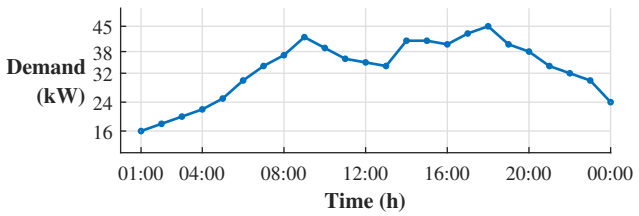


Fig. 6. The demand profile of the network in the first scenario

TABLE II. MGs' contribution in supplying the network demand in the first scenario of centralized operation mode (The MG' contribution is the multiplication of on/off status and generation level of each DER.)

| period (h) | MG1 (kW) | MG2 (kW) | MG3 (kW) | period (h) | MG1 (kW) | MG2 (kW) | MG3 (kW) |
|---|---|---|---|---|---|---|---|
| **1** | 15 | 0 | 1 | **13** | 15 | 4 | 15 |
| **2** | 15 | 0 | 3 | **14** | 15 | 11 | 15 |
| **3** | 15 | 0 | 5 | **15** | 15 | 11 | 15 |
| **4** | 15 | 0 | 7 | **16** | 15 | 10 | 15 |
| **5** | 15 | 0 | 10 | **17** | 15 | 13 | 15 |
| **6** | 15 | 0 | 15 | **18** | 15 | 15 | 15 |
| **7** | 15 | 4 | 15 | **19** | 15 | 10 | 15 |
| **8** | 15 | 7 | 15 | **20** | 15 | 8 | 15 |
| **9** | 15 | 12 | 15 | **21** | 15 | 4 | 15 |
| **10** | 15 | 9 | 15 | **22** | 15 | 2 | 15 |
| **11** | 15 | 6 | 15 | **23** | 15 | 0 | 15 |
| **12** | 15 | 5 | 15 | **24** | 15 | 0 | 9 |

TABLE III. Operation cost of MGs in the first scenario of centralized operation mode

| MG No. | Classical computing (Gurobi) | Iterations | Quantum computing | Iterations |
|---|---|---|---|---|
| MG1 | \$3281.99 | – | \$3281.98 | – |
| MG2 | \$3560.74 | – | \$3560.71 | – |
| MG3 | \$3247.88 | – | \$3247.86 | – |
| Total | \$10090.61 | 8 | \$10090.55 | 3 |

Gurobi.

According to Table III, the QC has a better computing performance compared to the classical counterpart, and can achieve the feasible solution in 3 iterations while the classical computing requires 8 iterations to get the same results as QC. As mentioned in subsection III-C, a successful approximation ratio of the objective function leads toward better optimization results using quantum algorithms. It is noted that the floating nature of cost coefficient $\alpha$ results in floating values for the objective function in Table III.

**Second scenario: Three DERs with demand change.** In this scenario, the load curve of the UC problem is decreased by 10 percent while other parameters are kept unchanged as the first scenario in the centralized UC problem. The contribution of each MG in centralized UC problem when the load curve is decrease by 10 percent can be seen in Table IV.

Compared to the first scenario, in Table IV, the power generation level of DERs is decreased when the total demand of microgrids is reduced by 10 percent. In this scenario, the operation cost of the network drops to \$9702, in which the operation cost of MG1, MG2 and MG3 is \$3279, \$3255 and \$3168, respectively.

**Third scenario: Nine DERs.** In the third scenario of centralized operation and optimization of microgrids, the number of DERs is increased in each microgrid. In this scenario, each MG consists of three dispatchable DERs.

As discussed in Section II-B, before converting integer variables to binary variables, there are 9 binary variables for commitment status of DERs, and 9 integer variables for the generation level of DERs at any given scheduling hour. After

This article has been accepted for publication in a future issue of this journal, but has not been fully edited. Content may change prior to final publication. Citation information: DOI 10.1109/TPWRS.2022.3141794, IEEE Transactions on Power Systems

TABLE IV. MGs' contribution in supplying the network demand in the second scenario of centralized operation mode (The MG' contribution is the multiplication of on/off status and generation level of each DER.)

| period (h) | MG1 (kW) | MG2 (kW) | MG3 (kW) | period (h) | MG1 (kW) | MG2 (kW) | MG3 (kW) |
|---|---|---|---|---|---|---|---|
| **1** | 14 | 0 | 0 | **13** | 15 | 1 | 15 |
| **2** | 15 | 0 | 1 | **14** | 15 | 7 | 15 |
| **3** | 15 | 0 | 3 | **15** | 15 | 7 | 15 |
| **4** | 15 | 0 | 5 | **16** | 15 | 6 | 15 |
| **5** | 15 | 0 | 8 | **17** | 15 | 9 | 15 |
| **6** | 15 | 0 | 12 | **18** | 15 | 11 | 15 |
| **7** | 15 | 1 | 15 | **19** | 15 | 6 | 15 |
| **8** | 15 | 3 | 15 | **20** | 15 | 4 | 15 |
| **9** | 15 | 8 | 15 | **21** | 15 | 1 | 15 |
| **10** | 15 | 5 | 15 | **22** | 15 | 0 | 14 |
| **11** | 15 | 2 | 15 | **23** | 15 | 0 | 12 |
| **12** | 15 | 2 | 15 | **24** | 15 | 0 | 7 |

conversion, since the generation level of each DER should be between 1kW and 15kW, we need $9\times15 = 135$ binary variables or qubits to cover the generation level limit at the corresponding scheduling hour. Therefore, to solve a simplified UC problem with nine DERs in the centralized operation mode by QAOA in each hour, we need $9 + 135 = 144$ binary variables or qubits, which exceeds the qubits availability in the quantum computers. Additionally, extra variables should be assigned to the slack variables to convert the inequality constraints to the equality constraints (first step of slack-based formulation in Section II.B.2). To overcome this drawback of current QC, this paper offers the idea of distributed operation and optimization of UC in the next subsection.

### *B. Distributed UC*

In the distributed UC, the main problem is separated into several subproblems, and each MG optimizes its objective function and only the joint variables are shared between entities to get the updated multiplier. To do this, the quantum ADMM developed in Section. III-B is used. In Fig. 7, the quantum distributed operation of MGs is shown, where each MGCC only shares the generated power value obtained by quantum optimization QAOA with each other to get the updated multipliers.

Here, the UC problem of nine DERs is split into three optimization subproblems, where each MG optimizes its UC problem consisting of three DERs. The characteristics of each DER are described in Table V. In the rest of this section, two different scenarios are tested.

**First scenario: Simplified distributed UC.** In this scenario, a simplified UC problem consisting of power generation capacity limit and power balance constraint is modeled.

In Table VI, the DERs' contributions in supplying the network demand are described after solving the UC problem consisting of nine DERs and three MGs. Fig. 8 shows the convergence speed of quantum-ADMM (Q-ADMM) compared to the classical version in terms of primal residuals.

As seen in Fig. 8, the computing performance of the ADMM algorithm is improved in quantum computing. The Q-ADMM can achieve the small primal residuals in less iterations compared to the classical ADMM.

**Second scenario: A real distributed UC problem without line power flow constraint.** In this scenario, unlike the simplified version of UC, other UC constraints are employed. These constraints are ramp-up, ramp-down, minimum up time, and minimum down time constraints. The ramp-up rate and ramp-down rate are adjusted to 1.6kW and 1.1kW, respectively. This scenario can show the performance of QC on a real power system UC problem. The problem input including power demand level and DER characteristics are as the first scenario. The contributions of each DER can be seen in Table VII. Comparing the results of first scenario (Table VI) and second

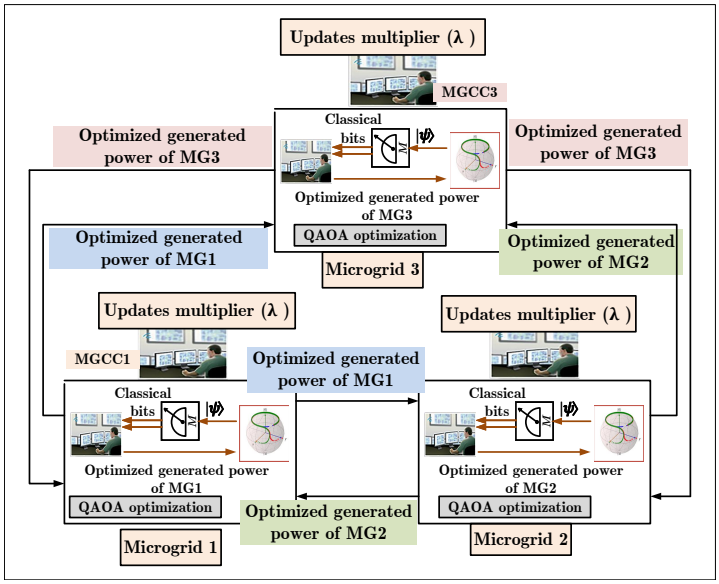


Fig. 7. Distributed operation mode of microgrids.

TABLE V. Characteristics of DERs in the distributed UC

| MG No. | DER No. | $\alpha$ | $\beta$ | $\gamma$ | $P^{min}$ | $P^{max}$ |
|---|---|---|---|---|---|---|
| MG1 | DER1 | 0.03 | 2 | 100 | 1kW | 15kW |
| | DER2 | 0.02 | 5 | 120 | 1kW | 15kW |
| | DER3 | 0.025 | 4 | 80 | 1kW | 15kW |
| MG2 | DER1 | 0.03 | 4 | 50 | 1kW | 15kW |
| | DER2 | 0.015 | 7 | 80 | 1kW | 15kW |
| | DER3 | 0.027 | 3 | 70 | 1kW | 15kW |
| MG3 | DER1 | 0.025 | 6 | 90 | 1kW | 15kW |
| | DER2 | 0.03 | 2 | 110 | 1kW | 15kW |
| | DER3 | 0.028 | 5 | 50 | 1kW | 15kW |

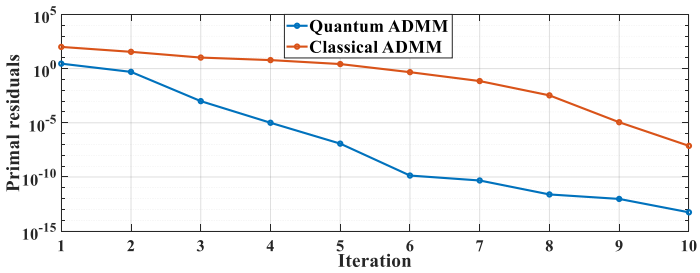


Fig. 8. Residual value of Q-ADMM and classical ADMM in distributed UC (first scenario)

TABLE VI. DERs' contribution in supplying the network demand in the simplified Distributed UC in presence of nine DERs using quantum-ADMM (first scenario)

| MG No. | DER No. | Scheduling time (h) | | | | | | | | | | | | | | | | | | | | | | | Total demand (kW) |
|---|---|---|---|---|---|---|---|---|---|---|---|---|---|---|---|---|---|---|---|---|---|---|---|---|---|
| | | 1 | 2 | 3 | 4 | 5 | 6 | 7 | 8 | 9 | 10 | 11 | 12 | 13 | 14 | 15 | 16 | 17 | 18 | 19 | 20 | 21 | 22 | 23 | 24 | |
| | | Generated power (kW) | | | | | | | | | | | | | | | | | | | | | | | | |
| MG1 | DER1 | 6.03 | 6.59 | 7.14 | 7.14 | 7.70 | 9.93 | 9.78 | 11.10 | 11.80 | 12.30 | 11.00 | 11.00 | 11.10 | 11.80 | 12.30 | 14.50 | 14.40 | 15.00 | 13.20 | 12.60 | 11.80 | 11.10 | 9.79 | 7.70 | 729.41 |
| | DER2 | 5.39 | 5.95 | 6.51 | 6.51 | 6.88 | 8.16 | 8.46 | 9.74 | 10.40 | 11.60 | 10.40 | 10.40 | 9.74 | 10.40 | 11.20 | 13.40 | 13.50 | 15.00 | 12.60 | 11.70 | 10.40 | 9.74 | 8.46 | 6.88 | |
| | DER3 | 5.60 | 6.16 | 6.71 | 6.71 | 7.19 | 8.32 | 8.75 | 9.26 | 11.20 | 11.80 | 10.90 | 10.90 | 9.27 | 11.20 | 12.30 | 12.80 | 13.70 | 15.00 | 12.80 | 12.20 | 11.20 | 9.27 | 8.76 | 7.19 | |
| MG2 | DER1 | 5.59 | 6.15 | 6.70 | 6.70 | 7.61 | 9.01 | 8.68 | 10.20 | 11.00 | 11.20 | 9.67 | 9.67 | 10.20 | 11.00 | 12.50 | 12.80 | 14.00 | 15.00 | 12.80 | 12.10 | 11.00 | 10.20 | 8.68 | 7.61 | 713.34 |
| | DER2 | 4.95 | 5.51 | 6.07 | 6.07 | 7.70 | 8.05 | 8.39 | 9.64 | 10.40 | 11.60 | 9.99 | 9.99 | 9.64 | 10.40 | 12.00 | 13.10 | 13.40 | 10.00 | 12.20 | 11.50 | 10.40 | 9.64 | 8.39 | 7.70 | |
| | DER3 | 5.82 | 6.38 | 6.93 | 6.93 | 8.24 | 8.67 | 8.91 | 10.10 | 11.30 | 11.20 | 10.80 | 10.80 | 10.10 | 11.40 | 12.60 | 13.10 | 14.30 | 15.00 | 13.00 | 12.40 | 11.30 | 10.10 | 8.91 | 8.25 | |
| MG3 | DER1 | 5.16 | 5.71 | 6.27 | 6.27 | 7.83 | 8.69 | 8.48 | 9.69 | 11.00 | 11.00 | 9.22 | 9.22 | 9.70 | 11.00 | 11.40 | 12.74 | 13.60 | 15.00 | 12.40 | 11.70 | 11.00 | 9.70 | 8.48 | 7.83 | 732.96 |
| | DER2 | 6.03 | 6.59 | 7.15 | 7.15 | 10.40 | 8.95 | 9.86 | 10.70 | 11.80 | 13.10 | 12.90 | 12.90 | 10.70 | 11.80 | 13.90 | 14.50 | 14.40 | 15.00 | 13.20 | 12.60 | 11.80 | 10.70 | 9.86 | 10.40 | |
| | DER3 | 5.37 | 5.93 | 6.48 | 6.48 | 6.42 | 8.28 | 8.65 | 9.53 | 11.00 | 11.10 | 10.10 | 10.10 | 9.53 | 11.00 | 11.80 | 12.80 | 13.70 | 15.00 | 12.60 | 12.00 | 11.00 | 9.53 | 8.65 | 6.43 | |
| Total power | | 50 | 55 | 60 | 60 | 70 | 78 | 80 | 90 | 100 | 105 | 95 | 95 | 90 | 100 | 110 | 120 | 125 | 130 | 115 | 109 | 100 | 90 | 80 | 70 | 2177 |
| cost | | 963 | 985 | 1008 | 1008 | 1052 | 1091 | 1099 | 1147 | 1194 | 1219 | 1166 | 1166 | 1147 | 1194 | 1241 | 1291 | 1317 | 1334 | 1268 | 1239 | 1194 | 1147 | 1099 | 1052 | - |

TABLE VII. DERs' contribution in supplying the network demand in a real distributed UC problem without line power flow constraint in presence of nine DERs using quantum-ADMM (second scenario)

| MG No. | DER No. | Scheduling time (h) | | | | | | | | | | | | | | | | | | | | | | | |
|---|---|---|---|---|---|---|---|---|---|---|---|---|---|---|---|---|---|---|---|---|---|---|---|---|---|
| | | 1 | 2 | 3 | 4 | 5 | 6 | 7 | 8 | 9 | 10 | 11 | 12 | 13 | 14 | 15 | 16 | 17 | 18 | 19 | 20 | 21 | 22 | 23 | 24 |
| | | Generated power (kW) | | | | | | | | | | | | | | | | | | | | | | | |
| MG1 | DER1 | 6.03 | 6.59 | 7.14 | 7.14 | 8.65 | 9.48 | 10.27 | 11.61 | 12.31 | 12.68 | 11.58 | 12.26 | 11.84 | 13.24 | 14.30 | 14.80 | 15.00 | 15.00 | 13.40 | 12.97 | 11.97 | 10.87 | 9.76 | 8.65 |
| | DER2 | 5.39 | 5.95 | 6.51 | 6.51 | 7.88 | 8.87 | 9.30 | 10.02 | 11.52 | 11.65 | 10.55 | 10.21 | 9.44 | 10.93 | 12.29 | 13.59 | 14.04 | 14.87 | 13.27 | 12.32 | 11.32 | 10.22 | 9.11 | 8.00 |
| | DER3 | 5.60 | 6.16 | 6.71 | 6.71 | 8.19 | 9.01 | 8.62 | 9.65 | 10.67 | 12.15 | 11.05 | 10.08 | 9.09 | 10.59 | 11.74 | 13.03 | 14.10 | 15.00 | 13.40 | 12.93 | 11.93 | 10.83 | 9.72 | 8.61 |
| MG2 | DER1 | 5.59 | 6.15 | 6.70 | 6.70 | 7.10 | 8.46 | 9.07 | 10.48 | 11.95 | 12.25 | 11.15 | 10.34 | 9.66 | 10.91 | 12.41 | 13.91 | 14.10 | 14.96 | 13.36 | 12.56 | 11.56 | 10.46 | 9.35 | 8.24 |
| | DER2 | 4.96 | 5.52 | 6.07 | 6.07 | 6.42 | 6.46 | 6.52 | 7.09 | 8.09 | 8.95 | 7.85 | 9.31 | 8.40 | 7.64 | 8.00 | 9.50 | 11.00 | 11.68 | 10.08 | 9.11 | 8.11 | 7.01 | 5.90 | 4.79 |
| | DER3 | 5.82 | 6.38 | 6.93 | 6.93 | 8.13 | 9.29 | 9.39 | 10.84 | 11.85 | 11.45 | 10.35 | 10.29 | 10.34 | 11.67 | 13.07 | 14.57 | 14.83 | 14.95 | 13.35 | 12.58 | 11.58 | 10.48 | 9.37 | 8.26 |
| MG3 | DER1 | 5.16 | 5.71 | 6.27 | 6.27 | 7.16 | 8.33 | 8.59 | 9.66 | 10.22 | 11.22 | 10.12 | 10.05 | 9.05 | 10.21 | 11.51 | 12.48 | 13.48 | 14.13 | 12.53 | 11.57 | 10.57 | 9.47 | 8.36 | 7.25 |
| | DER2 | 6.03 | 6.59 | 7.15 | 7.15 | 8.48 | 9.39 | 9.15 | 10.65 | 12.13 | 13.35 | 12.25 | 12.49 | 13.13 | 14.53 | 14.98 | 14.94 | 15.00 | 15.00 | 13.40 | 13.14 | 12.14 | 11.04 | 9.93 | 8.82 |
| | DER3 | 5.37 | 5.93 | 6.48 | 6.48 | 7.80 | 8.70 | 9.08 | 9.98 | 11.23 | 11.28 | 10.18 | 9.98 | 9.03 | 10.26 | 11.69 | 13.17 | 13.44 | 14.40 | 12.80 | 11.83 | 10.83 | 9.73 | 8.62 | 7.51 |

TABLE VIII. DERs' contribution in supplying the network demand in a real distributed UC including all constraints in presence of nine DERs using quantum-ADMM (third scenario)

| MG No. | DER No. | Scheduling time (h) | | | | | | | | | | | | | | | | | | | | | | | |
|---|---|---|---|---|---|---|---|---|---|---|---|---|---|---|---|---|---|---|---|---|---|---|---|---|---|
| | | 1 | 2 | 3 | 4 | 5 | 6 | 7 | 8 | 9 | 10 | 11 | 12 | 13 | 14 | 15 | 16 | 17 | 18 | 19 | 20 | 21 | 22 | 23 | 24 |
| | | Generated power (kW) | | | | | | | | | | | | | | | | | | | | | | | |
| MG1 | DER1 | 6.03 | 7.01 | 7.54 | 7.54 | 8.39 | 9.79 | 10.19 | 11.64 | 11.95 | 12.70 | 12.01 | 11.75 | 11.65 | 12.31 | 11.93 | 11.56 | 12.00 | 11.00 | 11.95 | 10.95 | 11.07 | 11.09 | 10.03 | 8.93 |
| | DER2 | 5.39 | 4.83 | 5.55 | 5.55 | 6.54 | 6.62 | 7.02 | 7.93 | 8.60 | 7.88 | 6.93 | 7.18 | 7.64 | 7.50 | 8.78 | 9.69 | 9.97 | 9.79 | 10.15 | 9.79 | 9.88 | 9.34 | 8.05 | 7.19 |
| | DER3 | 5.60 | 6.66 | 6.65 | 6.65 | 7.94 | 9.43 | 9.73 | 11.07 | 10.87 | 10.70 | 9.93 | 10.02 | 10.93 | 10.86 | 10.29 | 9.61 | 9.33 | 9.99 | 10.43 | 10.00 | 9.84 | 9.66 | 8.60 | 7.50 |
| MG2 | DER1 | 5.59 | 6.80 | 6.92 | 6.92 | 7.95 | 9.41 | 9.33 | 10.82 | 10.50 | 9.89 | 10.76 | 10.20 | 10.98 | 10.92 | 10.33 | 9.68 | 9.59 | 9.96 | 9.47 | 9.97 | 10.12 | 11.25 | 10.19 | 9.10 |
| | DER2 | 4.96 | 5.26 | 5.89 | 5.89 | 7.33 | 7.60 | 7.87 | 8.27 | 7.87 | 8.49 | 7.75 | 8.15 | 7.30 | 7.14 | 8.49 | 9.00 | 8.90 | 9.36 | 9.11 | 9.36 | 9.44 | 8.64 | 7.58 | 6.10 |
| | DER3 | 5.82 | 6.50 | 7.15 | 7.15 | 8.18 | 9.62 | 9.94 | 11.25 | 11.09 | 10.65 | 11.50 | 11.42 | 10.68 | 10.57 | 10.36 | 9.99 | 10.20 | 10.20 | 9.64 | 10.20 | 9.97 | 11.15 | 10.09 | 9.00 |
| MG3 | DER1 | 5.16 | 6.08 | 6.55 | 6.55 | 7.52 | 7.62 | 7.27 | 7.73 | 7.88 | 8.80 | 8.43 | 8.76 | 8.06 | 8.01 | 7.44 | 8.42 | 9.58 | 9.54 | 9.61 | 9.55 | 9.54 | 8.86 | 7.80 | 6.71 |
| | DER2 | 6.03 | 5.91 | 7.26 | 7.26 | 8.39 | 9.89 | 10.06 | 11.42 | 11.49 | 11.33 | 12.08 | 11.73 | 11.02 | 11.02 | 10.73 | 11.02 | 10.35 | 10.41 | 10.38 | 10.42 | 10.54 | 10.87 | 9.81 | 8.71 |
| | DER3 | 5.37 | 5.93 | 6.49 | 6.49 | 7.73 | 8.01 | 8.57 | 9.86 | 9.72 | 9.56 | 10.61 | 10.78 | 10.59 | 11.66 | 11.64 | 11.03 | 10.09 | 9.75 | 9.25 | 9.76 | 9.58 | 8.91 | 7.85 | 6.75 |

TABLE IX. Comparison of Operation cost of MGs in distributed operation mode in a real UC problem without line power flow constraint (second scenario)

| MG No. | Classical computing (Gurobi) | Quantum computing |
|---|---|---|
| MG1 | $10151.54 | $10151.53 |
| MG2 | $8019.50 | $8019.48 |
| MG3 | $9321.41 | $9321.40 |
| Total | $27492.45 | $27492.41 |

TABLE X. Operation cost of MGs in different operation modes

| Method | Scenario 1 | Scenario 2 | Scenario 3 |
|---|---|---|---|
| Centralized computing (Gurobi) | $27621.24 | $27492.45 | $28962.19 |
| Quantum ADMM | $27621.23 | $27492.41 | $28962.18 |

scenario (Table VII) demonstrates the impact of power ramp rate constraints, where differentiate the optimized generation level of DERs in different scheduling hours.

Table IX demonstrates the operation cost of microgrids for a real UC problem subject to power ramp rate and minimum up time and down time constraints in the distributed operation of microgrids.

**Third scenario: A real distributed UC problem including line power flow constraint.** In this scenario, the distributed UC problem including the line power flow limit is solved [35]. Table VIII is provided to describe the contribution of each DER after solving distributed UC in presence of all constraints including the line power flow constraint.

According to Table X, three different scenarios of distributed UC are considered to compare the obtained operation cost of microgrids by Q-ADMM with those results obtained by Gurobi solver in the centralized operation mode of microgrids so that the ADMM method is not involved.

## V. Discussion on quantum optimization

In this section, we briefly discuss current capabilities and barriers of quantum computing especially in solving quantum optimization problems:

- *Qubit connectivity.* In quantum algorithm development, the ideal qubit connectivity is considered in corresponding quantum circuit. In an ideal qubit connectivity, multi-qubit quantum gates are allowed to be operated between any existing qubits. Fig. 1 shows the connectivity graph $G$ of all-to-all connected devices. However, in reality, the physical architectures almost allows two-qubit operations between limited qubits, which necessitates surplus routing

operations or teleportation protocols. Therefore, the circuit depth will increase. To deal with this issue, co-design of quantum algorithms as well as quantum hardware is an active research area. To this end, error correction is considered in developing quantum algorithms as well as building quantum computers [36].

- *Number of qubits.* The number of qubits is one of the important factors in determining the size of the problem. At this time, IBM quantum machine, namely IBM Quantum Manhattan with 65 qubits, is a real machine with highest qubit number. Moreover, according to the road map of IBM, 1000-qubit machine, called IBM Quantum Condor will be developed until the end of 2023 [8]. This advancement in quantum machine technology can fully realize the quantum supremacy over classical computing.

## VI. Conclusion

This paper devised a quantum distributed method to solve the unit commitment problem in quantum computing framework. The quantum formulation of UC problem was further presented to prepare the subproblems for distributed optimization. The results showed that the idea of quantum distributed operation can successfully solve the UC problem in presence of more DERs than the quantum centralized optimization. However, in the distributed version, the number of subproblems should be in accordance to the available qubits. Comparing the obtained results with those from its classical counterpart ensured the superiority of QC in terms of computing performance.

Although, current noisy intermediate-scale quantum computers are using limited qubits in the computation process and only a small number of operations can be handled, our paper is a crucial step to push the frontier in solving the power system problems in a quantum architecture. The future work could investigate the application of quantum computing on stochastic analysis of power system reliability and optimization.

## References


[1] L. Wu, M. Shahidehpour, and T. Li, "Stochastic security-constrained unit commitment," *IEEE Transactions on Power Systems*, vol. 22, no. 2, pp. 800–811, 2007.

[2] S. Woerner and D. J. Egger, "Quantum risk analysis," *npj Quantum Information*, vol. 5, p. 15, 2019.

[3] S. Nauerth, F. Moll, M. Rau, C. Fuchs, J. Horwath, S. Frick, and H. Weinfurter, "Air-to-ground quantum communication," *Nature Photonics*, vol. 7, pp. 382–386, 2013.

[4] J. Shi, S. Chen, Y. Lu, Y. Feng, R. Shi, Y. Yang, and J. Li, "An approach to cryptography based on continuous-variable quantum neural network," *Scientific Reports*, vol. 10, p. 2107, 2020.

[5] B. P. Lanyon, J. D. Whitfield, G. Gillett, M. E. Goggin, M. P. Almeida, I. Kassal, J. Biamonte, M. Mohseni, B. J. Powell, M. Barbieri, A. Aspuru-Guzik, and A. G. White, "Towards quantum chemistry on a quantum computer," *Nature Chemistry*, vol. 2, pp. 106–111, 2010.

[6] J. Biamonte, P. Wittek, N. Pancotti, P. Rebentrost, N. Wiebe, and S. Lloyd, "Quantum machine learning," *Nature*, vol. 549, pp. 195–202, 2017.

[7] J. Preskill, "Quantum Computing in the NISQ era and beyond," *Quantum*, vol. 2, p. 79, 2018.

[8] National Academies of Sciences, Engineering, and Medicine, *Quantum computing: progress and prospects*. National Academies Press, 2019.

[9] J.-H. Bae, P. M. Alsing, D. Ahn, and W. A. Miller, "Quantum circuit optimization using quantum karnaugh map," *Scientific Reports*, vol. 10, p. 15651, 2020.

[10] E. Farhi, J. Goldstone, and S. Gutmann, "A quantum approximate optimization algorithm," *arXiv:1411.4028*, 2014.

[11] A. Gilliam, S. Woerner, and C. Gonciulea, "Grover adaptive search for constrained polynomial binary optimization," *arXiv:1912.04088*, 2019.

[12] E. Farhi, J. Goldstone, and S. Gutmann, "A quantum approximate optimization algorithm applied to a bounded occurrence constraint problem," *arXiv:1412.6062*, 2014.

[13] L. K. Grover, "A fast quantum mechanical algorithm for database search," in *Proceedings of the twenty-eighth annual ACM symposium on Theory of computing*, 1996, pp. 212–219.

[14] Z. Jiang, E. G. Rieffel, and Z. Wang, "Near-optimal quantum circuit for grover's unstructured search using a transverse field," *Physical Review A*, vol. 95, no. 6, p. 062317, 2017.

[15] G. G. Guerreschi and A. Y. Matsuura, "Qaoa for max-cut requires hundreds of qubits for quantum speed-up," *Scientific Reports*, vol. 9, p. 6903, 2019.

[16] D. J. Egger, J. Mareček, and S. Woerner, "Warm-starting quantum optimization," *Quantum*, vol. 5, p. 479, 2021.

[17] E. C. Finardi and E. L. da Silva, "Solving the hydro unit commitment problem via dual decomposition and sequential quadratic programming," *IEEE transactions on Power Systems*, vol. 21, no. 2, pp. 835–844, 2006.

[18] Y. Fu, M. Shahidehpour, and Z. Li, "Long-term security-constrained unit commitment: hybrid dantzig-wolfe decomposition and subgradient approach," *IEEE Transactions on Power Systems*, vol. 20, no. 4, pp. 2093–2106, 2005.

[19] S. Boyd, N. Parikh, and E. Chu, *Distributed optimization and statistical learning via the alternating direction method of multipliers*. Now Publishers Inc, 2011.

[20] P. Ramanan, M. Yildirim, N. Gebraeel, and E. Chow, "Large-scale maintenance and unit commitment: A decentralized subgradient approach," *IEEE Transactions on Power Systems*, 2021.

[21] X. Sun, P. B. Luh, M. A. Bragin, Y. Chen, J. Wan, and F. Wang, "A novel decomposition and coordination approach for large day-ahead unit commitment with combined cycle units," *IEEE Transactions on Power Systems*, vol. 33, no. 5, pp. 5297–5308, 2018.

[22] Y. Xue, Z. Li, C. Lin, Q. Guo, and H. Sun, "Coordinated dispatch of integrated electric and district heating systems using heterogeneous decomposition," *IEEE Transactions on Sustainable Energy*, vol. 11, no. 3, pp. 1495–1507, 2020.

[23] N. Moll, P. Barkoutsos, L. S. Bishop, J. M. Chow, A. Cross, D. J. Egger, S. Filipp, A. Fuhrer, J. M. Gambetta, M. Ganzhorn *et al.*, "Quantum optimization using variational algorithms on near-term quantum devices," *Quantum Science and Technology*, vol. 3, no. 3, p. 030503, 2018.

[24] K. Tanahashi, S. Takayanagi, T. Motohashi, and S. Tanaka, "Application of ising machines and a software development for ising machines," *Journal of the Physical Society of Japan*, vol. 88, no. 6, p. 061010, 2019.

[25] A. Lucas, "Ising formulations of many np problems," *Frontiers in Physics*, vol. 2, p. 5, 2014.

[26] S. Kumar, H. Zhang, and Y.-P. Huang, "Large-scale ising emulation with four body interaction and all-to-all connections," *Communications Physics*, vol. 3, no. 1, pp. 1–9, 2020.

[27] S. Boettcher, "Analysis of the relation between quadratic unconstrained binary optimization and the spin-glass ground-state problem," *Phys. Rev. Research*, vol. 1, p. 033142, 2019.

[28] S. Karimi and P. Ronagh, "Practical integer-to-binary mapping for quantum annealers," *Quantum Information Processing*, vol. 18, pp. 1–24, 2019.

[29] B. Jiang, T. Lin, S. Ma, and S. Zhang, "Structured nonconvex and nonsmooth optimization: algorithms and iteration complexity analysis," *Computational Optimization and Applications*, vol. 72, no. 1, pp. 115–157, 2019.

[30] M. X. Goemans and D. P. Williamson, "Improved approximation algorithms for maximum cut and satisfiability problems using semidefinite programming," *Journal of the ACM (JACM)*, vol. 42, no. 6, pp. 1115–1145, 1995.

[31] A. W. Harrow and A. Montanaro, "Quantum computational supremacy," *Nature*, vol. 549, no. 7671, pp. 203–209, 2017.

[32] B. M. Terhal and D. P. DiVincenzo, "Adaptive quantum computation, constant depth quantum circuits and arthur-merlin games," *arXiv preprint quant-ph/0205133*, 2002.

[33] A. P. Lund, M. J. Bremner, and T. C. Ralph, "Quantum sampling problems, bosonsampling and quantum supremacy," *npj Quantum Information*, vol. 3, no. 1, pp. 1–8, 2017.

[34] D. E. Olivares, C. A. Cañizares, and M. Kazerani, "A centralized energy management system for isolated microgrids," *IEEE Transactions on Smart Grid*, vol. 5, no. 4, pp. 1864–1875, 2014.

[35] B. Lu and M. Shahidehpour, "Unit commitment with flexible generating units," *IEEE Transactions on Power Systems*, vol. 20, no. 2, pp. 1022–1034, 2005.

[36] C. Wilen, S. Abdullah, N. Kurinsky, C. Stanford, L. Cardani, G. d'Imperio, C. Tomei, L. Faoro, L. Ioffe, C. Liu *et al.*, "Correlated charge noise and relaxation errors in superconducting qubits," *Nature*, vol. 594, no. 7863, pp. 369–373, 2021.

This article has been accepted for publication in a future issue of this journal, but has not been fully edited. Content may change prior to final publication. Citation information: DOI 10.1109/TPWRS.2022.3141794, IEEE Transactions on Power Systems

**Nima Nikmehr** (Senior Member, IEEE) is currently working toward the Ph.D. degree in electrical engineering with the department of Electrical and Computer Engineering, Stony Brook University, Stony Brook, NY, USA. His research interests include power system optimization, networked microgrids and quantum computing.

**Peng Zhang** (M'07−SM'10) received the Ph.D. degree in electrical engineering from the University of British Columbia, Vancouver, BC, Canada, in 2009. He is a Professor of Electrical and Computer Engineering, and a SUNY Empire Innovation Professor at Stony Brook University, New York. He has a joint appointment at Brookhaven National Laboratory as a Staff Scientist. Previously, he was a Centennial Associate Professor and a Francis L. Castleman Associate Professor at the University of Connecticut, Storrs, CT, USA. He was a System Planning Engineer at BC Hydro and Power Authority, Canada, during 2006-2010. His research interests include AI-enabled smart grids, quantum-engineered power grids, networked microgrids, power system stability and control, cybersecurity, and formal methods and reachability analysis.

Dr. Zhang is an individual member of CIGRÉ. He is an Editor for the IEEE Transactions on Power Systems, the IEEE Power and Energy Society Letters, and the IEEE Journal of Oceanic Engineering.

**Mikhail A. Bragin** Mikhail A. Bragin (Member: IEEE, PES, INFORMS) is an Assistant Research Professor in the Department of Electrical and Computer Engineering at the University of Connecticut. His research work has been supported by the U.S. National Science Foundation, BNL, MISO, ISO-NE, ABB, CESMII, and AFRL. His research is geared toward solving complex technical and societal challenges within smart grids, supply chains, and artificial intelligence. Accordingly, his research interests include operations research, mathematical optimization, including power system optimization, grid integration of renewables (wind and solar), energy-based operation optimization of distributed energy systems, stochastic scheduling within manufacturing systems, and machine learning through deep neural networks. His research has appeared in top journals such as *Journal of Optimization Theory and Applications*, *IEEE Transactions on Power Systems*, *IEEE Transactions on Automation Science and Engineering*, *Decision Support Systems* and *IEEE Robotics and Automation Letters* as well as in top conferences such as *PES General Meeting*, *INFORMS Annual Meeting* and *International Joint Conference on Artificial Intelligence*.